Heritage Science

RESEARCH ARTICLE

Open Access

Indian Ocean trade connections: characterization and commercial routes of torpedo jars

Silvia Lischi[1], Eleonora Odelli[1,2], Jhashree L. Perumal[3], Jeannette J. Lucejko[4], Erika Ribechini[4], Marta Mariotti Lippi[5], Thirumalini Selvaraj[3], Maria Perla Colombini[4] and Simona Raneri[6*]

Abstract

During the Classical Period (300 BC–400 AD), the Indian Ocean emerged as one of the largest hubs of ancient international trade. For a long period, these contacts were described from a Rome-centric point of view, looking at the connections between Rome and India. However, recent studies have demonstrated that the Roman-Indo connection was only one of the vast medium and short distance trade routes involving numerous regions and populations, exchanging goods and culture. Current archaeological investigations have demonstrated that several minor trade dynamics formed the primary connective tissue of the Indian Ocean. This study attempts to trace these mid-range connections by focusing on the transport of torpedo jars, recently found in several settlements throughout the Indian Ocean. Two archaeological sites were considered: Al Hamr al-Sharqiya 1 (Inqitat, southern Oman), and the port of Alagankulam (southern India). An analytical protocol based on thin sections analysis, SEM–EDS, XRD and GC/MS was applied to a selection of fragments from the two archaeological sites. The analytical investigation carried out on these vessels identified three different ceramic compositions, which distributed differently in the two sites, characterized by a black coating due to a similar bitumen source. The location of the production sites and comparative studies between these vessels and reference materials available in the literature enabled us to cast new light on the routes followed by the torpedo jars, from Mesopotamia to India and Oman.

Keywords: Indian Ocean routes, Torpedo jars, Multi-analytical techniques, GC/MS, XRD, Bitumen

Introduction

The study of the commercial contacts between Rome and India originated with the excavation of Arikamedu by Sir Mortimer Wheeler [1]. The classification of numerous archaeological materials as originating from the Mediterranean promoted several studies regarding the Roman domination or colonization of the Indian coasts [2–5], reinforcing the idea of the Roman control of the Indian Ocean trade.

This Rome-centric point of view remained almost unchanged until the end of the 1980s, and the archaeological campaign carried out in Arikamedu by Begley [6, 7]. However, the trade between Rome and India was only one of numerous connections within the Indian Ocean over long, medium and short distances. These interactions were not limited to goods trade but also, and above all, to exchanges in cultural habits, language and traditions.

These connections in the Indian Ocean involved a very large area, including the Red Sea, East Africa, the Persian Gulf, Southern Arabia and India [8–10]. This network connected people from all the coasts of the Indian

*Correspondence: simona.raneri@unipi.it
[6] National Research Council, ICCOM-CNR, Pisa Research Area, Via Moruzzi 1, Pisa, Italy
Full list of author information is available at the end of the article

Lischi *et al. Herit Sci*   (2020) 8:76

Page 2 of 14

Ocean and beyond, trading in aromatics, textiles, spices, precious stones, slaves, grain and an incredible range of other commodities and substances [11].

Based on the literature and archaeological evidence, from ancient times there were two main routes through the Indian Ocean, namely the Persian Gulf and the Red Sea [12]. In the 5th millennium BC there are traces of small networks, navigating along the coast of the Indian Ocean [13, 14]. From the Hellenistic period, thanks to Alexander the Great and his campaign in India (327 BC), the trade from the Indian Ocean reached the Eastern Mediterranean through Antioch or Gaza [12]. After the conquest of Egypt by the Romans in 30 BC, traders began to reach the Mediterranean also through the Red Sea.

Although some of these connections have begun to be studied, the extent and reasons for these trades are still an open issue. Other aspects also need to be taken into consideration. Firstly, the climate of most of the regions bordering the Indian Ocean means that many of the materials involved in these trades have not been preserved, making it difficult to quantify how often such trade took place. Many organic materials, for example, are only preserved in particularly dry climatic conditions, such as in the Red Sea [15–17]. In addition, the common practices of reusing and recycling [18] make it impossible to conduct qualitative or quantitative analyses of the contents of the jars. Ceramics are the most valuable material for such analysis; in fact, some ceramic vessels were not used very frequently (they break easily), the fragments do not have many potential uses and are therefore thrown away. In archaeological contexts these vessels are normally well preserved [19].

Of the ceramics that act as tracers of the Indian Ocean trade, torpedo jars are an excellent material with easily recognizable characteristics. They represent a class of transport vessels that were widely diffused throughout the Indian Ocean over a relatively long-time interval (1st–10th AD) [19].

The name of these containers comes from their shape; in fact, they are tall and long, they have no handles, a narrow mouth and a pointed base [19]. For a long time, they were regarded as Roman amphorae, due to their similarities with LR1 types [20] and their similar use [21]. However, the internal brownish-blackish coating always attributed to bitumen facilitates their identification [20]. This material was poured into the vessel in liquid form, swilled around inside and the remainder poured out [22]. Traces of this waterproofing process are sometimes visible in the incrustation of bitumen running down the rim of some sherds. Bituminous materials have been widely used in the Middle Eastern regions, thanks to their easy availability [23]. Bitumen is an organic fossil material derived from petroleum surface outcrops. It has a chemical composition that varies according to the area of origin, genesis and age. By characterizing the bituminous traces in the vessels, it is possible to hypothesize the area of origin, and thus understand the provenance of the archaeological artefact under study. The trade route that the artefact travelled along can then be established, and thus the trade routes of a certain historical period and a geographical area [24].

Torpedo jars were likely produced in Mesopotamia, although there is no evidence of kilns. They were used as liquid containers, probably for wine. They have been found along the coast of the Indian Ocean through the Persian Gulf [25]. In spite of few archaeometric studies [25], their classification is mainly based on the typology, thus differentiating between TORP.S—brownish orange in color with abundant, well-sorted, mixed sandy grit inclusions—and TORP.C—creamy in color with less sand inclusions [26]. Based on their distribution and frequency in archeological sites during the Late Antiquity and Early Islamic periods (3rd–9th cent. AD), TORP.S seems to be overtaken by TORP.C around the mid-to late 8th century. However, this classification remains limited to the typological classification, without the definition of clear compositional reference groups; additionally, literature studies didn't analyze the Classical period [19, 20], investigated in the present research.

This study analyzes two sets of torpedo jars from two different sites in the Indian Ocean both active during the Classical Period, 300 BC–AD 400 [27, 28], and representing important harbors and entrepôt of the Indian Ocean (Fig. 1, Table 1): the port of Alagankulam [29] in the Gulf of Mannar, southern India (fourteen samples) and the site of Al Hamr al-Sharqiya 1 [27, 30] on the promontory of Inqitat, Dhofar, southern Oman (four samples).

The minero-petrographic analysis of the ceramic paste, in depth analysis of specific tempers and chemical fingerprint of bitumen using well established analytical procedures [31, 32] enabled us to propose new clues on the circulation and use of this type of container, traded from Mesopotamia to what is nowadays referred to as Oman and south-eastern India, thus extending the current knowledge on the medium range commercial circuits within the Indian Ocean.

Methods

Minero-petrographic analyses and SEM

Thin sections were studied under a light microscope and a petrographic description was carried out following the Whitbread classification criteria [33]. X-ray diffraction (XRD) analysis was performed on a few grammes of powered samples using a Bruker D2 PHASER diffractometer in the following experimental conditions: 4°—65° 2θ, with a 0.02° 2θ step size and a counting time of 184.5 s per
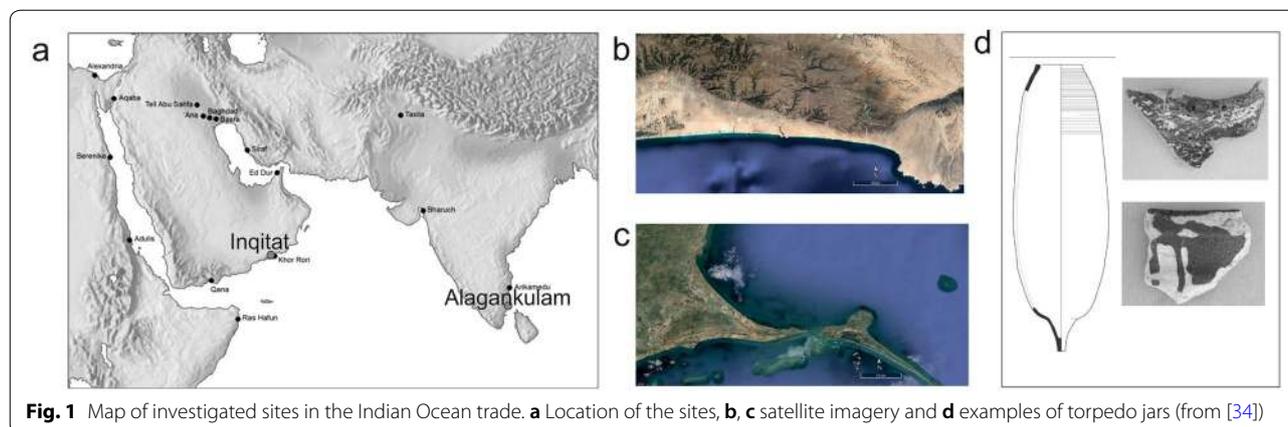
Lischi *et al. Herit Sci* (2020) 8:76

Page 3 of 14

Fig. 1 Map of investigated sites in the Indian Ocean trade. **a** Location of the sites, **b**, **c** satellite imagery and **d** examples of torpedo jars (from [34])

Table 1 Samples and analytical techniques applied

Site	Sample ID	Colour (Munsell Index [55])	Optical microscopy	XRD	SEM	GC/MS
Alagankulam, South-east India	AMG1	5 YR 8/4	+			+
	AGM2	5 YR 7/4	+			+
	AGM3	5 YR 8/3 Note: not visible residue	+			–
	AGM4	5 YR 7/6 Note: not visible residue	+			–
	AGM5	5 YR 7/4	+	+		+
	AGM6	5 YR 8/4	+			+
	AGM7	5 YR 8/4	+	+		+
	AGM8	10 YR 7/2	+		+	+
	AGM9	5 YR 8/3	+			+
	AGM10	10 YR 7/2	+	+		+
	AGM11	5 YR 8/3	+	+		+
	AGM12	10 YR 7/3 Note: not visible residue	+	+		–
	AGM13	5 YR 8/4	+		+	+
	AGM14	10 YR 7/4	+	+		+
Al Hamr al-Sharqiya 1 on Inqitat	OM1	10 YR 7/4	+	+		+
	OM2	10 YR 7/3	+	+	+	+
	OM3	10 YR 7/3	+	+		+
	OM4	10 YR 7/3	+	+		+

Reference samples of bitumen were also analyzed; bitumen sample from Babylonia area was provided by Dr Esaim Fadhel Khalfa from the University of Babylon, Iraq and sample from Middle East (Judea) came from Kremer Pigmente GmbH (Germany)

step; tube current and voltage: 30 mA and 40 kV, respectively. Micromorphological observations were carried out on small chips of samples using a ZEISS Supra55VP SEM-EDS with a patented "in-lens" Schottky Field Emission Gun (FEG) equipped with a Bruker EDS system.

Plant temper analysis
The plant tempers were identified by observation of thin sections under a light microscope. The plant tempers were measured, and their morphology compared with

the literature [34–36] and reference fresh samples of *O. sativa,* which were collected in southern Tuscany, sectioned with a cryotome, stained with toluidine blue, and observed under a light microscope.

GC/MS equipment and sample preparation
The GC/MS instrumentation consists in a 6890 N Network GC System (Agilent Technologies, Palo Alto, CA, USA) equipped with a PTV injector and coupled to a 5975 Mass Selective Detector with quadrupole analyser.

Lischi *et al. Herit Sci*   (2020) 8:76

Page 4 of 14

MS parameters: electron impact ionization (EI, 70 eV) in positive mode; ion source temperature 230 °C; scan range 50–700 m/z; interface temperature 280 °C. GC separation was performed on an HP-5MS column (J&W Scientific, Agilent Technologies, stationary phase 5% phenil–95% methylpolysiloxane, 30 m length, 0.25 mm i.d., 0.25 µm film thickness) connected to a deactivated fused silica precolumn (J&W Scientific, Agilent Technologies, 2 m length, 0.32 mm i.d.). GC program for the: 80 °C, for 2 min isothermal, 20 °C/min up to 200 °C, 4 °C/min up to 300 °C, isothermal for 60 min. He flows 1.2 ml/min, injector temperature 280 °C. Amorphous black residue collected from the ceramic fragments as well as the reference bitumen from areas in Babylonia and Judea were subjected to a sample pre-treatment in order to identify free alkanes, aromatic and polar compounds of bituminous materials [31]. The bitumen sample from the Babylonia area was provided by Dr Esaim Fadhel Khalfa from the University of Babylon (Iraq) and the sample from Middle East (Judea) came from Kremer Pigmente GmbH (Germany).

Each archaeological sample (ca. 10 mg) was extracted using 1 mL of an extractant solvent mixture consisting in n-hexane, dichloromethane and methanol (in the ratios 80:15:5, v/v/v) in a microwave oven (MLS-1200 MEGA Milestone) for five minutes (power 500 W, temperature 60 °C). The extract was centrifuged at 2000 rpm for five minutes, and the supernatant was evaporated to dryness under a nitrogen stream. A total of 300 µL of hexane was added, and the solution was sonicated for five minutes at 40 °C to allow asphaltene precipitation ($\times$ 3 times). Starting from the deasphalted solution, the saturated and aromatic hydrocarbons were separated from the polar fraction, using column chromatography with silica gel activated at 400 °C prior to use. Saturated and aromatic hydrocarbons were eluted with 3 mL of n-hexane: dichloromethane (1:1, v/v). The fraction containing the saturated and aromatic hydrocarbons was dried under a nitrogen stream and re-dissolved in 50 µL of isooctane. A total of 2 µL of the final solution was analyzed by GC/MS.

Results

Minero-petrographic characterization

The thin section analysis of jars from the two investigated sites enabled us to identify three main petrographic fabrics. Fabric A includes only samples from Alagankulam and is characterised by metamorphic and volcanic rock fragments. Fabric B comprises jars from both Alagankulam and Al Hamr al-Sharqiya 1 and is characterized by the presence of fibers as tempers. Fabric C comprises just one sample—from

Alagankulam—and is characterized by quartz fragments and abundant microfossil tests (*foraminifera*).

The jars in Fabric A (samples A1, A2, A5, A6, A7, A9, A11, A13, A14, Fig. 2a, b) are characterized by a clayey matrix, from red to orange in color, scarcely micaceous, with low-medium/locally absent, optical activity. The microstructure is mainly due to irregular voids, some of which are due to fossil molds, reaching a diameter of 500–700 µm. Only in samples A11, A6, and A14 were observed elongated preferential oriented voids, of up to 100 µm in length. The aplastic fraction (average diameter 100–200 µm) is due to fractured quartz (locally polycrystalline), feldspar (some altered), plagioclase, pyroxenes, micas, flint fragments, amphibole, and rare siltstones, with a unimodal grain size distribution. Volcanic glass fragments are also present. Amorphous concentration features (ACFs) are present.

Fabric B includes two samples from Alagankulam (A8, A12, Fig. 2c) and four samples from Al Hamr al-Sharqiya 1 (O1, O2, O3, O4 Fig. 2d, e). They are characterized by a clayey matrix, ochre yellowish in color, with low/absent optical activity. The microstructure is due to elongated voids with an opening of about 100–150 µm, mainly due to plant temper residues. Irregular voids are also present. The matrix is highly depurated, exhibiting ultra-fine aplastic fragments (< 100 µm), mainly due to quartz.

Finally, sample A10 (Fabric C, Fig. 2f) is characterized by a clayey matrix, ochre yellowish in color, with no optical activity. The microstructure is due to scarce spherical voids, mainly due to fossil molds. Irregular voids are also present, reaching 800 µm in length. Some of the bigger pores are filled with secondary calcite. Abundant fossil fragments due to planktonic foraminifera are visible. The aplastic fraction is fine (100–300 µm), ranging from rounded to sub-angular in shape; fragments are due to highly fractured quartz, feldspars, sericite and micas.

The mineralogical composition of the all ceramics was investigated by X-ray diffraction analysis. The results obtained (Table 2) confirm the petrographic observation, with interesting clues as to the firing temperatures. Specifically, in samples from Fabrics B and C, the detection of a small amount of mullite along with a large amount of gehlenite, anorthite and diopside (not present as tempers and thus useful as firing temperature indicators [37, 38]) suggest the use of Ca-rich kaolinite-based clays fired at high temperatures (> 900 °C). The samples from Fabric A, suggest the use of illite-based clays, without mineralogical clues regarding the firing temperature as the main temperature indicators are present as tempers, according to thin section observations.
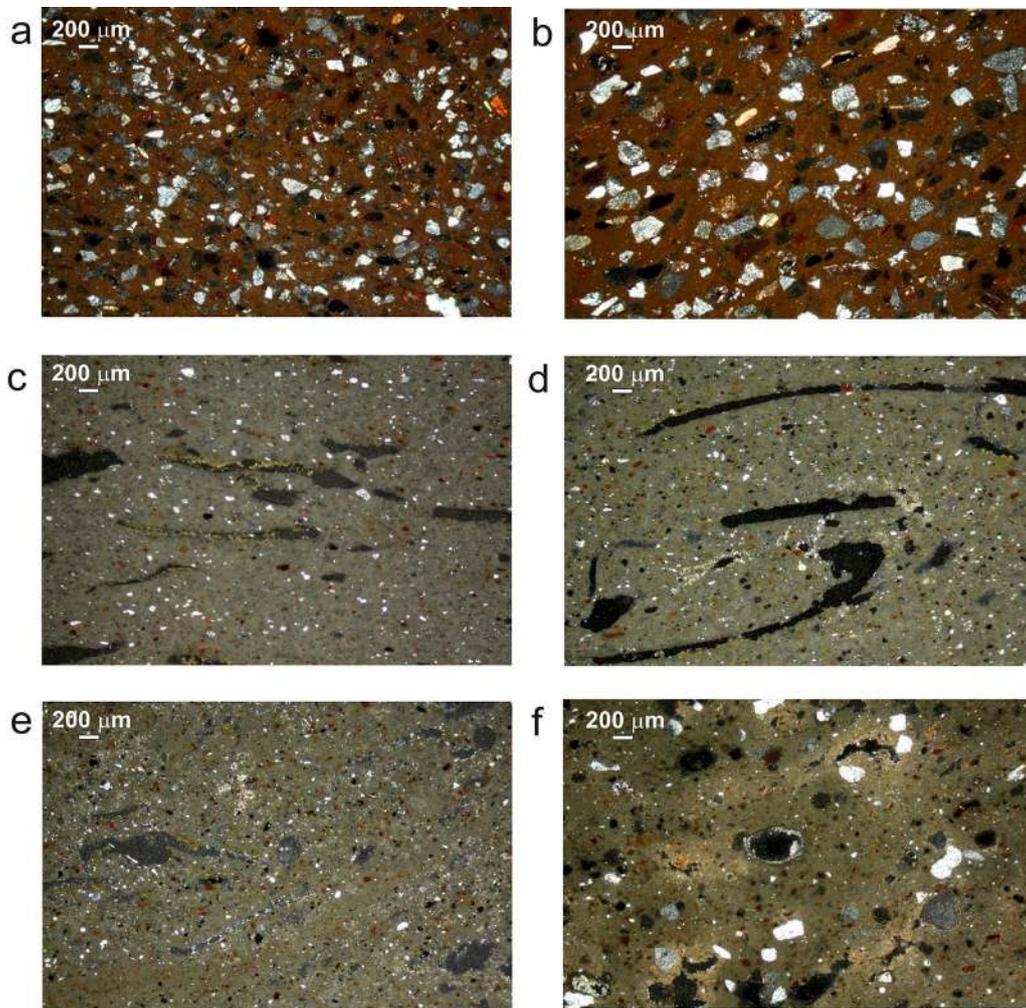
Lischi *et al. Herit Sci*   (2020) 8:76

Page 5 of 14

Fig. 2 Microphotographs of samples representative of the identified petrographic fabrics. Fabric A: samples **a** A5 and **b** A13; Fabric B: samples **c** A8, **d** O1, **e** O3; Fabric C, sample **f** A10

Table 2 Semi-quantitative data on mineral phases detected by XRD analysis

Sample ID	Fabric	Quartz	Albite	Amphibole	Anortihte	Diopside	Gehlenite	Illite/ muscovite	Mullite	Hematite
AGM 5	Fabric A	xx	x	x	xx	x	–	x	–	–
AGM7	Fabric A	xx	x	x	xx	x	–	x	–	–
AGM11	Fabric A	xx	x	x	xx	x	–	x	–	–
AGM14	Fabric A	xx	x	x	xx	x	–	x	–	–
AGM12	Fabric B	xx	–	–	x	x	xx	–	tr	x
OM1	Fabric B	xx	–	–	x	xx	x	–	tr	x
OM2	Fabric B	xx	–	–	x	xx	x	–	tr	x
OM3	Fabric B	xx	–	–	x	xx	x	–	tr	x
OM4	Fabric B	xx	–	–	x	xx	x	–	tr	x
AGM10	Fabric C	xx	–	–	x	x	tr	tr	tr	x

(x) is related to the relative phase abundance; tr = traces

Lischi *et al. Herit Sci*   (2020) 8:76

Page 6 of 14

Micromorphological analysis by scanning electron microscope

SEM observations were carried out in order to investigate the extent of vitrification of the clay paste. They support hypotheses regarding firing temperatures based on thin section and XRD analysis [39]. One representative sample of each petrographic fabric and site excavation was examined, as representative of the compositional variability. The micro-morphological investigation (Fig. 3) indicated that in all the analyzed samples the matrix shows from initial vitrification to complete vitrification. This would seem to confirm the high temperature ranges suggested by the low-absent optical activity of the matrix observed in the thin section and by the mineralogical composition, when Ca–Al–silicate firing indicators were present as newly-formed minerals (in Fabric B and C).

Analysis of plant temper

The organic inclusions observed in the thin sections of Fabric B were interpreted as plant tempers (Fig. 4). These mainly consisted of linear or curved whitish strips of different lengths, sometimes u-shaped and often tapering at the ends, resembling sections of leaf-like structures. Most display a wavy edge opposite a straight edge, with a thickness spanning from about 80 μm in the crests to about 40 μm in the troughs. The distance between the crests is variable, averaging about 70 μm. The edges of a few strips are both straight. One

or two of the tips of the strips are often curled. The strips appeared to be cavities, rather than actual plant remains. The cellular structure was not preserved. Small portions of tissue showed barely visible cell outlines in the cavity left by the oxidation of the temper elements.

Plant tempers were very badly preserved possibly because they had been severely affected by oxidation during firing. Organic materials are normally destroyed after firing at high temperatures; only phytoliths, which are commonly found in the plant tempers, may tolerate temperatures up to 500 °C without visible deformations [40]. As a consequence, the Fabric B temper and reference material were compared on the basis of the general shape of the inclusions. In fact, the outline and the size of the plant temper varied according to the cutting plane of the ceramic thin section, which cut the leaf-like structures in different orientations. In any case this analysis showed a good similarity between the temper of Fabric B and the rice chaff (*Oryza sativa* L.). The temper elements with a straight edge and a wavy edge could be interpreted as transversal or oblique sections of a lemma or a palea, which both show a smooth adaxial surface and abaxial surface characterized by alternating furrows and ridges oriented according to the main axis of the bract, which have curled or slightly curled edges. The elements with both edges straight could be longitudinal sections of the same bracts, most
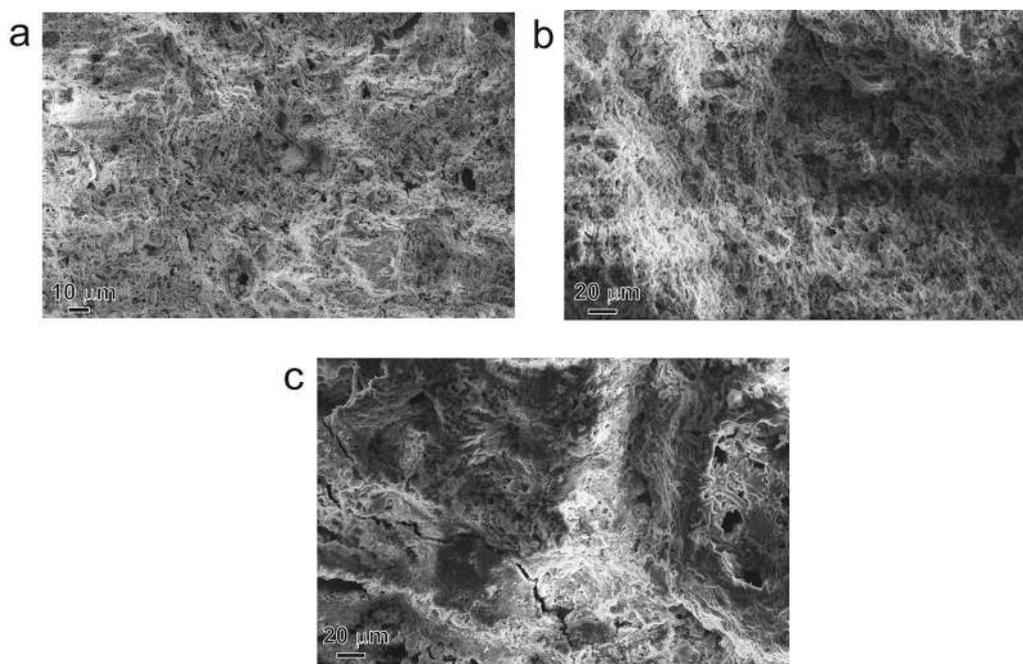

Fig. 3 SEM images of ceramic microstructures in samples **a** A13, **b** A8, **c** O2

Lischi *et al. Herit Sci*   (2020) 8:76
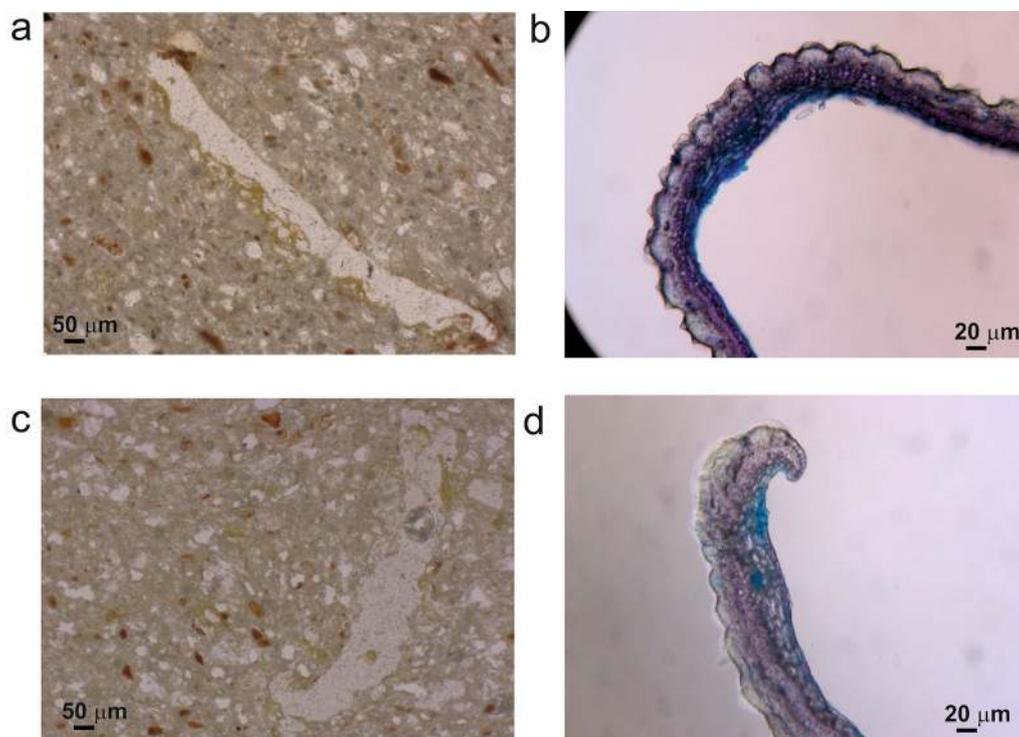
Page 7 of 14

Fig. 4 Plant tempers in Fabric B samples. **a** Plant temper in AMG8. Note the occurrence of a straight edge and an opposite wavy edge. **b** Transversal section of a lemma of *O. sativa*. **c** Plant temper with curled tip in OM1. **d** Curled margin of a lemma of *O. sativa*. Transversal section

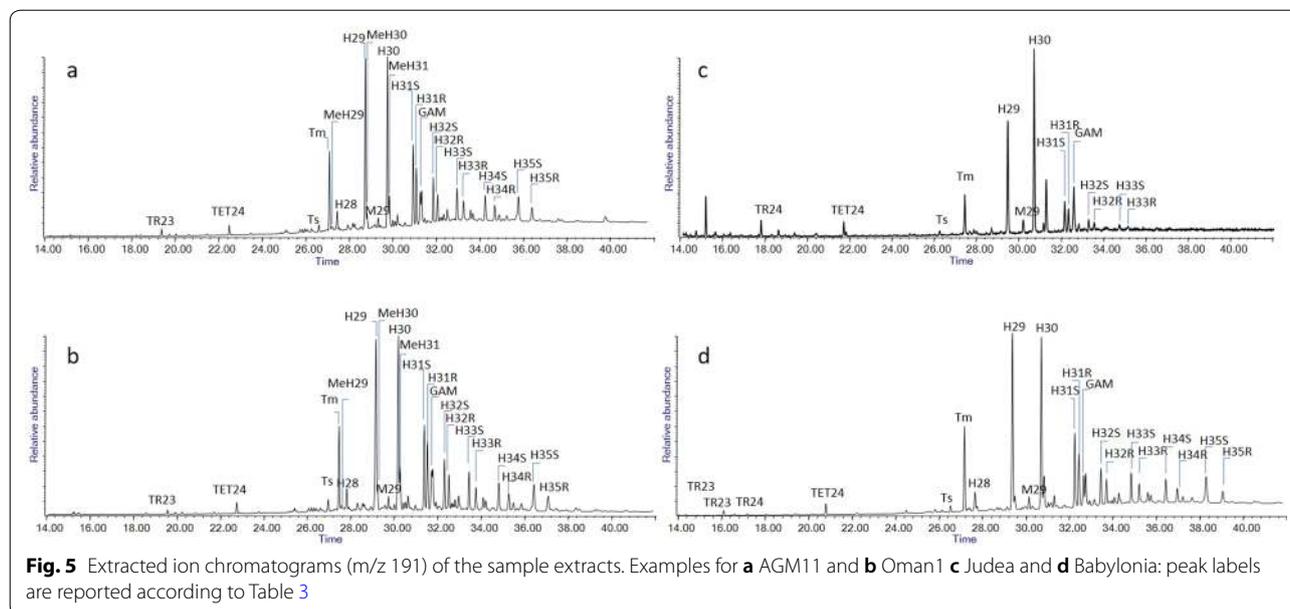probably in the furrows because ridges present rows of tubercles, or sections of the glumes, which have smooth surfaces.

The plants that were used as temper are characterized by a notable amount of silica; whose accumulation is particularly enhanced in Poales [41]. This could partly explain the large use of cereal byproducts in tempering ceramics. In fact, cereal crop processing produces abundant waste, which consists of different plant portions, mainly stalks, husks and ear bristles. The availability of cereal processing byproducts is related to cereal cultivation; therefore, their addition to the clay paste indicates the occurrence of cereal farming in the geographical area of production of the artifacts. Given that different cereal crops are characteristic of different cultural areas, the plant temper may denote the origin of the ceramic materials [42].

GC/MS analysis of black coatings

The chromatographic profiles obtained from the analysis of the samples collected from Algankulam (India) and Al Hamr al-Sharqiya 1 (Oman) are very similar. Figure 5a, b shows the results for sample A11 from India, and O1 from Oman, while Table 3 lists all the compounds identified in all the chromatograms.

Chromatographic data indicate the occurrence of bitumen in all the samples analysed. The most abundant peaks in the extracted ion chromatograms of m/z 191 are due to $17\alpha(H),21\beta b(H)$-30-Norhopane (H29) and $17\alpha(H),21\beta(H)$-Hopane (H30). $17\alpha(H),18\alpha(H),21\beta(H)$-28,30-Bisnorhopane (H28), $17\beta(H),21\alpha(H)$-Hopane (M30) and Gammacerane (GAM) are present in high abundances, followed by $17\beta(H),21\alpha(H)$-30-Norhopane (M29). The benzohopane BHC35 and the tricyclic terpane series (TR23, TR24, TR25) as well as tetracyclic terpane (TET24) are present in low abundances. The chromatographic profiles show the entire series of Homohopanes (H31-H35). The relative abundance of homohopane compounds decreases as the number of carbon atoms increases. The two isomers Ts $(18\alpha(H),21\beta(H)$-22,29,30-Trisnorhopane) and Tm $(17\alpha(H),18\alpha(H),21\beta(H)$-22,29,30-Trisnorhopane) are also present, the second one in much greater abundance than the first. $18\alpha(H)$- and $18\beta(H)$-oleanane was detected only in some profiles with a very low abundance (sample A8, A10 and all the Oman samples).

The GC/MS profiles obtained for samples from both archaeological sites were compared to reference bitumen from Judea and Babylonia areas (Fig. 5c, d), as well as different sources of bitumen and different geographical

Lischi *et al. Herit Sci*   (2020) 8:76

Page 8 of 14

Fig. 5 Extracted ion chromatograms (m/z 191) of the sample extracts. Examples for **a** AGM11 and **b** Oman1 **c** Judea and **d** Babylonia: peak labels are reported according to Table 3

areas such as those from the Dead Sea, Abu Jir, Hit [23] and Iraq [43]. The comparison highlighted a great similarity with bitumen sources from the Babylonia area (reference material) and Abu Jir or Hit, which are today part of Iraq [23].

Aromatic steranes are present in all the samples analysed with low or very low abundances (Fig. 6), highlighting severely altered steranes. The decreasing homohopane series and low and very low steranes can be attributed to the biodegradation [23] of bituminous material.

In order to identify the bitumen source, parameters from the literature were used to compare and evaluate the origin, biodegradation and age of different bitumen sources [44]. Table 4 reports the biomarker ratios calculated for all samples analysed.

Low values of Ts/Tm ratio < 0.5 indicate a marine carbonate depositional environment [45]. Low gammacerane index values were observed, such as GAM/H30 (Gammacerane/17α(*H*),21β(*H*)-Hopane) and GAM/H31R (Gammacerane/22*R*-30-Homohopane), the first ranging from 0.16 to 0.28 and the second from 0.51 to 0.70 (see Table 3). These indicate that our bitumen samples were formed in reducing conditions in different saline depositional environments, which were mainly marine carbonate [44, 46]. All the samples from both archaeological sites showed a high ratio of H29/H30, with values greater than 1, ranging from 1.01 to 1.39, indicating a marine environment with organic rich carbonates [47]. The predominance of H29-Norhopane is consistent with a carbonate source rock [45]. Also, the H35/H34 index with values higher than 0.8 indicates a marine

carbonate or evaporite environment [44]. Analysed samples produced values of 1.02–1.64, indicating a hypersaline, anoxic carbonate environment of deposition with no available free oxygen. In addition, the bisnorhopane index (H28/H30) with the low/medium values indicates a source rock with a marine carbonate environment [45].

The Ts/Tm ratio is one of the indices that has been used to characterize and evaluate the thermal deposition maturity. In our case the values of this index are low but very similar, indicating that Tm is dominant. Low values indicate low maturities [44]. Another ratio obtained from bitumen biomarkers used to indicate the maturity of the source rocks is the 2α-methylhopane index, which is strongly affected by the burial temperature [48]. The immature source usually has a low index value. In our case the low values obtained, between 0.19 and 0.40, further confirm the immature source rocks for both the archaeological bitumen from Algankulam and Al Hamr al-Sharqiya 1.

The chemical composition, thermal maturity and type of source rocks of the bitumen samples from India were very similar to those from Oman (see Table 4). Figure 7 compares various characteristic parameters, such as the Ts/Tm index of maturity, indexes of gammacerane variation GAM/H31R, GAM/H30 and ratio of redox conditions H29/H30 obtained for samples from the two analysed sites and those for the reference bitumen from various natural deposits. All the samples were very similar to bitumen from Hit, Abu Jir, Iraq [23, 46] and Babylonia. On the other hand, bitumen from Judea and the Dead Sea [23] show different profiles and thus different biomarker ratios.

Lischi *et al. Herit Sci*   (2020) 8:76

Page 9 of 14

Table 3 List of the compounds identified in the bitumen samples analyzed by GC–MS procedure

TR23	C23 Tricyclic terpane
TR24	C24 Tricyclic terpane
TR25	C25 Tricyclic terpane
TET24	C24 Tetracyclic terpane
Ts	18α(*H*),21β(*H*)-22,29,30-Trisnorhopane
Tm	17α(*H*),18α(*H*),21β(*H*)-22,29,30-Trisnorhopane
MeH29	2α-methyl-17α(*H*),21β(*H*)-30-Norhopane
H28	17α(*H*),18α(*H*),21β(*H*)-28,30-Bisnorhopane
C29stig	C29-20S-5α(*H*),14α(*H*),17α(*H*)-Stigmastane
	C29-20R-5α(*H*),14β(*H*),17β(*H*)-Stigmastane
	C29-20S-5α(*H*),14β(*H*),17β(*H*)-Stigmastane
	C29-20R-5α(*H*),14α(*H*),17α(*H*)-Stigmastane
H29	17α(*H*),21β(*H*)-30-Norhopane
MeH30	2α-methyl-17α(*H*),21β(*H*)-Hopane
C29Ts	17α(*H*),21β(*H*)-30-Norneohopane
M29	17β(*H*),21α(*H*)-30-Norhopane (normoretane)
OL	18α(*H*)- and 18β(*H*)-oleanane
H30	17α(*H*),21β(*H*)-Hopane
MeH31	2α-methyl-17α(*H*),21β(*H*)-30-Homohopane
H31S	22S-17α(*H*),21β(*H*)-30-Homohopane
MeH32	2α-methyl-17α(*H*),21β(*H*)-30,31-Bishomohopane
H31R	22R-17α(*H*),21β(*H*)-30-homohopane
GAM	Gammacerae
H32S	22S-30,31-Bishomohopane
H32R	22R-30,31-Bishomohopane
H33S	22S-17α(*H*),21β(*H*)-30,31,32-Trishomohopane
H33R	22R-17α(*H*),21β(*H*)-30,31,32-Trishomohopane
H34S	22S-17α(*H*),21β(*H*)-30,31,32,33-Tetrakishomohopane
H34R	22R-17α(*H*),21β(*H*)-30,31,32,33-Tetrakishomohopane
H35S	22S-17α(*H*),21β(*H*)-30,31,32,33,34-Pentakishomohopane
H35R	22R-17α(*H*),21β(*H*)-30,31,32,33,34-Pentakishomohopane
BHC35	C35 Benzohopane
S22	C21 5α(*H*),14α(*H*),17α(*H*)-sterane
C27ααS	C27 20S-5α(H),14α(H),17α(H)-cholestane
C27ββR	C27 20R-5α(H),14β(H),17β(H)-cholestane
C27ββS	C27 20S-5α(H),14β(H),17β(H)-cholestane
C27ααR	C27 20R-5α(H),14α(H),17α(H)-cholestane
C28ααS	C28 20S-5α(H),14α(H),17α(H)-ergostane
C28ββR	C28 20R-5α(H),14β(H),17β(H)-ergostane
C28ββS	C28 20S-5α(H),14β(H),17β(H)-ergostane
C28ααR	C28 20R-5α(H),14α(H),17α(H)-ergostane
C29ααS	C29 20S-5α(H),14α(H),17α(H)-stigmastane
C29ββR	C29 20R-5α(H),14β(H),17β(H)-stigmastane
C29ββS	C29 20S-5α(H),14β(H),17β(H)-stigmastane
C29ααR	C29 20R-5α(H),14α(H),17α(H)-stigmastane

Discussion and conclusions

This research provides, for the first time, a systematic compositional and technological classification of various classes of torpedo jars, which all show evidence of a common production area in Mesopotamia. Specifically, the GC/MS analysis of the black coating locates the production of all the studied torpedo jars to the area of Iraq, as resulted from the comparison of GC/MS profile with reference data (see Fig. 7). The differences detected by the minero-petrographic analysis suggest a complex scenario encompassing different production workshops in Mesopotamia, from which different jars batches were exported through different routes.

Based on our investigations, two classes and three different petrographic fabrics were identified among the studied torpedo jars; the first characterized by orange color and grit inclusions due to volcanic-metamorphic tempers (Fabric A) which occurs only in Alagankulam (India); the second characterized by a creamy color with less inclusions, discriminated in two petrographic fabrics namely a fiber tempered one (Fabric B) occurring both in Alagankulam (India) and in Al Hamr al-Sharqiya 1 (Oman) and a fossiliferous rich one (Fabric C) typical only of Alagankulam (India).

Fabric A might be associated with TORP.S type; it is reported as a pre-mid-8th cent. production [26] which is coherent with the Alagankulam stratigraphic sequence. In a moment when the Alagankulam harbor took the role as the main entrepôt in south-India in commercial contacts with Sri Lanka (e.g., Thissamaharama), a direct route from Iraq to India probably existed for the TORP.S jars. In India, the literature reports several examples of torpedo jars characterized by rock fragment tempers with a mineralogical assemblage due to volcanic and metamorphic fragments. Looking at the Persian Gulf area, this compositional fingerprint could be associated with clay sources located in the north of Baghdad [25, 49], in accordance with studies which locates their source areas within the southern Zagros mountains [26]. In this investigation, no records of TORP.S were found in Al Hamr al-Sharqiya 1 (Oman); in 8th cent. the Al Hamr al-Sharqiya 1 site had already been destroyed and abandoned since some centuries. Nevertheless, it is possible that this type of ceramic was present in the assemblage of HAS2 [27], an entrepôt in the northeastern area of Inqitat; however, no potteries from this settlement have yet been analyzed [50].

Fabric B and C might be interpreted as TORP.C type, due to their creamy color and the few sandy inclusions. Based on the literature, the mid-8th cent. marks the transition between TORP.S (orange-red with grit inclusions) and TORP.C (creamy vessels) [26]; however, this is in contradiction with the Al Hamr al-Sharqiya 1 sequence which date the fiber-tempered creamy typology (Fabric B) to 1st–2nd centuries AD, as well as with records from Egypt, at Myos Hormos, or from Sumhuram, in Oman,
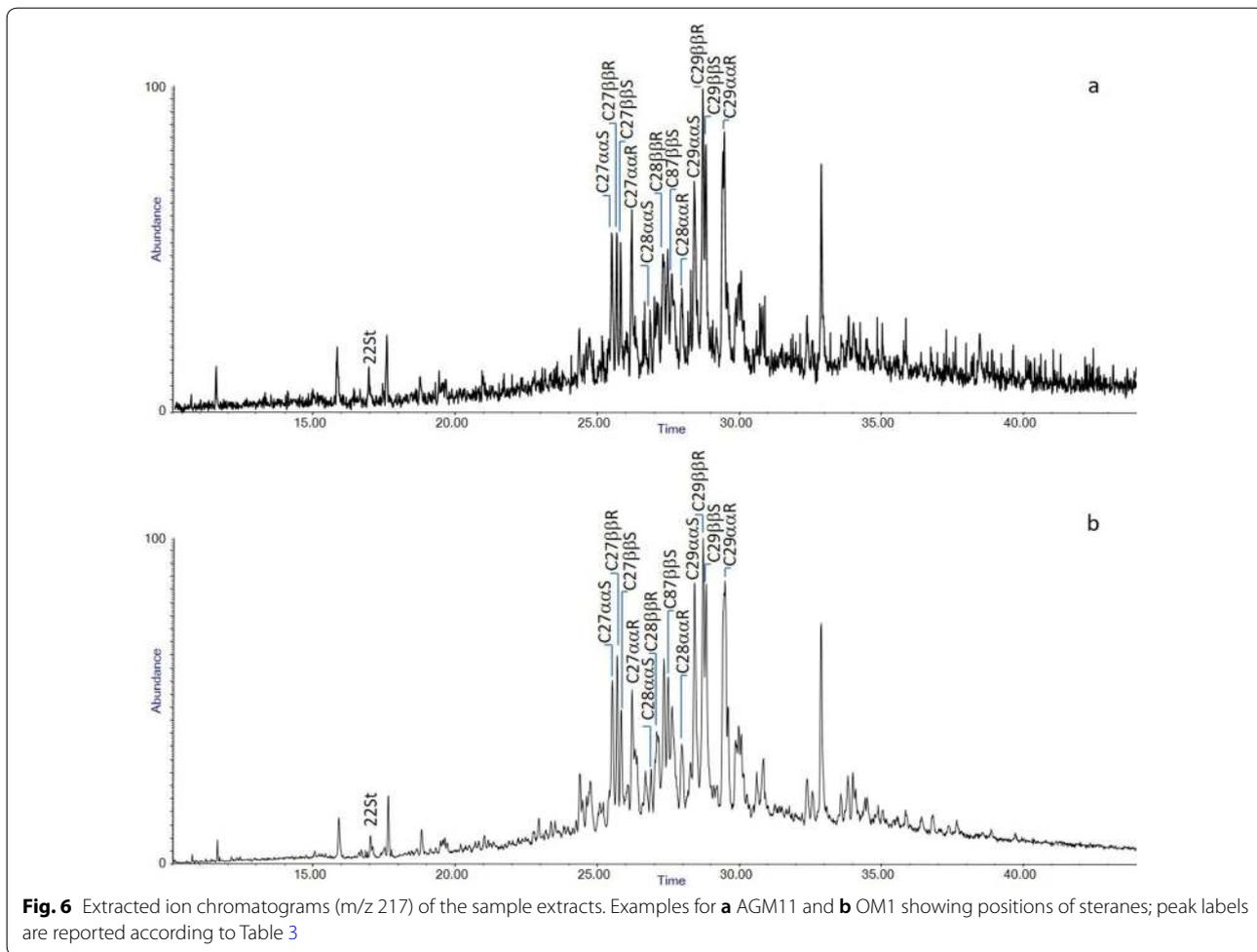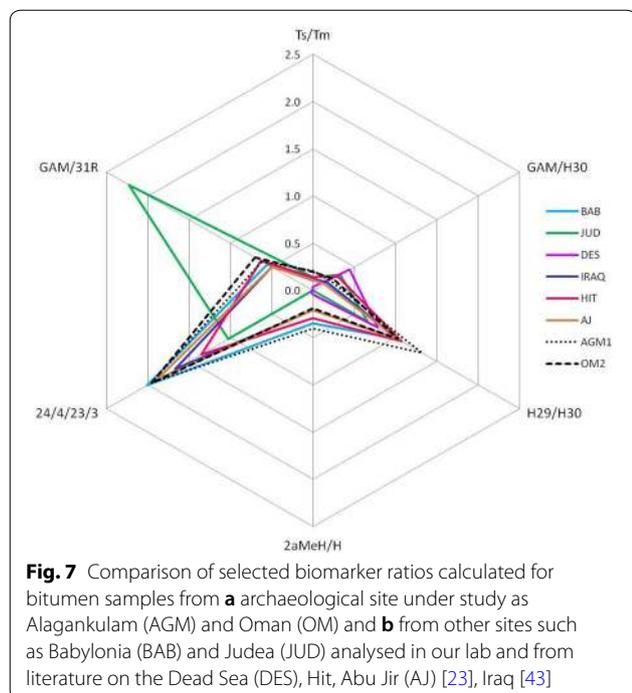
Fig. 6 Extracted ion chromatograms (m/z 217) of the sample extracts. Examples for **a** AGM11 and **b** OM1 showing positions of steranes; peak labels are reported according to Table 3

Table 4 Biomarker ratios

Site	Sample ID	Ts/Tm	GAM/H30	GAM/H31R	H29/H30	H35/H34	H28/H30	2aMeH/H	24/4/23/3
Alagankulam, South-East India	AGM1	0.2	0.2	0.6	1.3	1.3	14.1	0.4	2.0
	AGM2	0.2	0.3	0.6	1.1	1.4	8.7	0.3	2.8
	AGM5	0.2	0.2	0.6	1.4	0.4	15.1	0.3	3.5
	AGM6	0.2	0.3	0.7	1.2	1.3	13.0	0.2	1.7
	AGM7	0.2	0.2	0.6	1.3	1.3	15.4	0.4	1.1
	AGM8	0.2	0.2	0.5	1.2	1.5	12.6	0.4	1.2
	AGM9	0.2	0.2	0.6	1.1	1.6	14.7	0.4	0.9
	AGM10	0.1	0.2	0.5	1.1	1.0	9.6	0.3	2.5
	AGM11	0.1	0.2	0.5	1.0	1.6	10.2	0.3	1.7
	AGM13	0.2	0.2	0.6	1.3	1.3	15.5	0.4	3.0
	AGM14	0.2	0.3	0.6	1.2	1.5	12.3	0.4	2.6
Al Hamr al-Sharqiya 1 on Inqitat	OM1	0.2	0.2	0.7	1.0	1.1	11.6	0.2	3.1
	OM2	0.2	0.3	0.7	1.0	1.2	11.6	0.2	2.0
	OM3	0.1	0.2	0.6	1.0	1.1	11.6	0.2	3.1
	OM4	0.1	0.3	0.7	1.0	1.2	8.5	0.2	4.1

Characteristic biomarker ratios calculated from the abundances of the various compounds detected in the extracted ion chromatograms (m/z 191) for samples from Alagankulam and from Al Hamr al-Sharqiya 1

Lischi *et al. Herit Sci*　　(2020) 8:76

Page 11 of 14

Fig. 7 Comparison of selected biomarker ratios calculated for bitumen samples from **a** archaeological site under study as Alagankulam (AGM) and Oman (OM) and **b** from other sites such as Babylonia (BAB) and Judea (JUD) analysed in our lab and from literature on the Dead Sea (DES), Hit, Abu Jir (AJ) [23], Iraq [43]

where similar containers occur in contexts datable, at least, to the 1st cent. AD [34, 51]. These evidences would suggest a scenario more complex than suggested in literature, so that the typology and the surface buff cannot be used as the solely chronological indicator.

As regards Fabric B samples, they have been found both in India and Oman from 1st to 2nd AD stratigraphic sequences; they were thus probably produced in antiquity and traded on multiple routes: a southern route from Mesopotamia to India and beyond, and a western route going from Oman (Al Hamr al-Sharqiya 1) to the Red Sea, in the direction of the Mediterranean Sea. It is therefore likely that a great diffusion occurred during the Sasanide period [25], but after the opening of the sea

route such containers began to transit along the Indian Ocean route to the east and west. Another interesting observation related to Fabric B potteries is the presence of rice chaff. The first evidence of rice in Mesopotamia dates back to the Hellenistic period [52, 53], but the only direct evidence currently available is from Susa [53] and can be traced back to the 1st cent AD. The chronology of this finding matches perfectly with the chronology of the torpedo jars we analyzed and seems to emphasize the presence of cultivated rice in the production area of Susa.

In respect to the creamy vessel characterized by foraminifera rich clay paste (Fabric C), it could be identified with another TORP.C type [26], later than the first typology; in fact, this creamy type is absent in the stratigraphic sequence of Inqitat, where nor Fabric C neither TORP.S were found. Otherwise, in Alagankulam, all the torpedo jars fabrics were herewith identified, confirming a long-lasting occupancy of the site and its relevant role in the Indian Ocean trade over a wide chronological interval (since 1st–2nd AD—marked by the presence of TORP.C/Fabric B—to post-mid-8th cent. AD—marked by the presence of TORP.S and the TORP.C/Fabric C type-; see Table 5). The composition of Fabric C type is, again, in accordance with the geological areas identified as torpedo jars sources, namely within the southern Zagros; in fact, geological outcrops bearing planktonic foraminifera have been identified in the Western Iraqi desert Paleocene sequences [54].

To sum up, the analysis of bitumen coatings suggest that the torpedo jars originated from a common area located in the area of Iraq, where different local raw materials and a common bitumen source were available (Fig. 8). The variability in minero-petrographic features would confirm the use of different sources from an area identified within the southern Zagros (through central and southern Iraq and southwest Iran), where both alluvia rich in volcanic and metamorphic rock fragments and Paleocene sequences bearing foraminifera were attested.

Table 5　Comparison of the nomenclatures and their chronology used in the literature with those reported in our work

Reference	This study	Priestman, 2013 [19]	Connan et al. 2020 [26]
Identified typology	Fabric A	TORP.RG 8th–10th cent. AD	TORP.S before 8th cent. AD
	Fabric B 3rd cent. BC–AD 3rd cent.	TORP.S 3rd cent. BC–AD 10th cent	?
	Fabric C		TORP.C 8th–10th cent. AD
Analysis	Typology Petrography GC/MS identification of bitumen sources	Typology	Typology GC/MS identification of 　bitumen sources Carbon isotope (δ^{13}C)

The analyses carried out to arrive at the results are also reported

Lischi *et al. Herit Sci*   (2020) 8:76

Page 12 of 14

Fig. 8 Reconstruction of the long-distance routes across the Indian Ocean, the Red Sea and the Persian Gulf. In red, the possible routes along which torpedo jars were distributed from Mesopotamia to Oman and India

The study provided the first petrographic classification of TORP.S types, which occurrence in Alagankulam sequence would be in accordance with the chronology reported in the literature (before the mid-8th cent.). Otherwise, in respect to the creamy fabrics (both fibers tempered and foraminifera rich clays), the obtained results dated back to 1st-2nd AD the plant-tempered TORP.C type, thus suggesting that the solely typological classification cannot be used as chronological indicator. In fact, the literature would date the TORP.C production after the mid-8th cent AD. It can be thus hypothesized that two types of TORP.C circulated in antiquity: a first type, credibly corresponding to Fabric B (fiber tempered) dated to 1st–2nd AD and a second type, which could correspond to Fabric C (fossil-rich paste) which might overtake the TORP.S type in the mid-8th cent. or coexist with TORP.S; however, a possible confirm of these hypotheses could be achieved only with the support of petrographic analysis on vessels from already studied pottery sequences.

Abbreviations
SEM–EDS: Scanning Electron Microscope–Energy Dispersion System; XRD: X ray diffraction; GC–MS: Gas Chromatography–Mass Spectrometry; BC: Before Christ; AD: Anno Domini; TORP.S: Torpedo jars Sandy, orange fine wares; TORP.RG: Torpedo jars Red Grit, cream coloured; HAS2: An entrepôt in the northeastern area of Inqitat; A(n): Samples from Alagankulam (India); O(n): Samples from Oman; ACF: Amorphous Concentration Feature; H28: 17α(*H*),18α(*H*),21β(*H*)-28,30-Bisnorhopane; H29: 17α(*H*),21βb(*H*)-30-Norhopane; H30: 17α(*H*),21β(*H*)-Hopane; M29: 17β(*H*),21α(*H*)-30-Norhopane; M30: 17β(*H*),21α(*H*)-Hopane; GAM: Gammacerane; BHC35: Benzohopane; TR23, TR24, TR25: Terpane series; TET24: Tetracyclic terpane;

H31-H35: Homohopanes; Ts: 18α(*H*),21β(*H*)-22,29,30-Trisnorhopane; Tm: 17α(*H*),18α(*H*),21β(*H*)-22,29,30-Trisnorhopane.

Author details
[1] Department of Civilizations and Forms of Knowledge, University of Pisa, Via dei Mille 19, 56126 Pisa, Italy. [2] Department of Archaeology, Ghent University, Sint-Pietersnieuwstraat 35, 9000 Ghent, Belgium. [3] Department of Structural and Geotechnical Engineering School of Civil Engineering, Vellore Institute of Technology, Vellore, India. [4] Department of Chemistry and Industrial Chemistry, University of Pisa, Via Moruzzi 13, 56124 Pisa, Italy. [5] Department of Biology, University of Florence, Via La Pira, 4, 50121 Florence, Italy. [6] National Research Council, ICCOM-CNR, Pisa Research Area, Via Moruzzi 1, Pisa, Italy.

Lischi *et al. Herit Sci*   (2020) 8:76

Page 13 of 14

References

1. Wheeler REM, Ghosh A, Krishna D. Arikamedu: an Indo-Roman trading station on the east coast of India. Ancient India. 1946;2:17–124.
2. Wheeler REM. Archaeology from the earth. Oxford: Clarendon Press; 1954.
3. Wheeler REM. Rome beyond the Imperial Frontiers. London: Bell; 1954.
4. Wheeler REM. Rome Beyond the Imperial Frontiers. London: Middlesex; 1955.
5. Wheeler REM. My Archaeological Mission to India and Pakistan. London: Thames and Hudson; 1976.
6. Begley V, Francis P, Mahadevan I. The Ancient Port of Arikamedu: New investigation and Researches 1989–1992. Pondicherry: Ecole Francaise D'Extreme-Orient; 1996.
7. Begley V, et al. The Ancient Port of Arikamedu: New Excavations and Researches, 1989–1992, vol. Two. Paris: Ecole Francaise D'Extreme-Orient; 2004.
8. Magee P. Revisiting Indian Rouletted Ware and the impact of Indian Ocean trade in Early Historic south Asia. Antiquity. 2010;84:1043–54.
9. Pavan A, Schenk H. Crossing the Indian Ocean before the Periplus: a comparison of pottery assemblages at the sites of Sumhuram (Oman) and Tissamaharama (Sri Lanka). Arab Archaeol Epigr. 2012;23:191–202.
10. Schenk H. Parthian glazed pottery from Sri Lanka and the Indian Ocean trade. Zeitschrift für Archäologie Außereuropäischer Kulturen. 2007;2:57–90.
11. Seland EH. Archaeology of Trade in the Western Indian Ocean, 300 BC–AD 700. J Archaeol Res. 2014;22:367–402.
12. Salles J-F. Tradition and Archaeology: Early Maritime Contacts in the Indian Ocean. New Delhi: Manohar; 1998.
13. Kitchen KA. The elusive land of Punt revised, in Trade and travel. In: Lunde P, Porter A, editors. The Red Sea region: proceedings of Red Sea project I, held in the British Museum. Oxford: Archaeo Press; 2004.
14. Ratnagar S. Trading Encounters: From the Euphrates to the Indus in the Bronze Age. Oxford: India Paperbacks; 2006.
15. Wild JP, Wild FC, Sidebotham SE, Wendrich WZ. Berenike 1999/2000: Report on the Excavations at Berenike, Including Excavations in Wadi Kalalat and Siket, and the Survey of the Mons Smaragdus Region. Berkeley: University of California; 2007. p. 225–227.
16. Peacock D, Blue L. Myos Hormos – Quseir al-Qadim: Roman and Islamic Ports on the Red Sea, Survey and Excavations 1999-2003. Oxford: Oxbow Books; 2006.
17. Handley F, Regourd A. Textiles with writing from Quseir al-Qadim – finds from the Southampton excavations 1999–2003. In: Blue L, Cooper J, Thomas R, Whitewright J, editors. Connected Hinterlands. Proceedings of Red Sea Project IV, held at the University of Southampton September 2008. British Archaeological Reports S2052 (International Series)/Society for Arabian Studies Monographs 8. Oxford: Archaeopress; 2009. p. 141–54.
18. Simpson St. J. Glass and small finds from Sasanian contexts at the ancient city-site of Merv. In: Nikonorov VP, ed. Central Asia from the Achaemenids to the Timurids. Archaeology, history, ethnology, culture. Materials of an international scientific conference dedicated to the centenary of Aleksandr Markovich Belenitsky, St. Petersburg: November 2–5, 2004. Institute of the History of Material Culture of the Russian Academy of Sciences, State Hermitage; 2004. p. 232–38.
19. Priestman, S.: A quantitative archaeological analysis of ceramic exchange in the Persian Gulf and Western Indian Ocean, AD c.400–1275. University of Southampton, Faculty of Humanities, Doctoral Thesis (2013) http://eprints.soton.ac.uk/id/eprint/370037. Accessed 15 May 2020.
20. Tomber R. Indo-Roman trade: from pots to pepper. London: Bristol Classical Press; 2008.
21. Simpson St. J. From Mesopotamia to Merv: reconstructing patterns of consumption. In: Potts T, Roaf M, Stei D, eds. Sasanian households, in Culture Through Objects. Ancient Near Eastern Studies in Honour of P.R.S. Moorey. Oxford: Griffith Institute; 2003. p. 347–75.
22. Stern B, Connan J, Blakelock E, Jackman R, Coningham RA, Heron C. From Susa to Anaradhapura: reconstructing aspects of trade and exchange in bitumen-coated ceramic vessels between Iran and Sri Lanka from the third to the ninth centuries AD. Archaeometry. 2008;50:409–28.
23. Connan J. Use and trade of bitumen in antiquity and prehistory: molecular archaeology reveals secrets of past civilizations. Philos Trans R Soc Lond B Biol Sci. 1999;354:33–50.
24. Connan, J., Van de Velde, T., An overview of bitumen trade in the Near East from the Neolithic (c.8000 BC) to the early Islamic period. Arabian Archaeology and Epigraphy, 2010; 21, 1-19.
25. Tomber R. Rome & Mesopotamia—importers into India in the first millennium AD. Antiquity. 2007;81:972–88.
26. Connan J, Priestman S, Vosmer T, Komoot A, Tofighian H, Ghorbani B, Engel MH, Zumberge A, van de Velde T. Geochemical analysis of bitumen from West Asian torpedo jars from the c. 8th century Phanom-Surin shipwreck in Thailand. J Archaeol Sci. 2020;117:105111.
27. Lischi S. Risultati preliminari delle ricerche archeologiche presso l'insediamento HAS1 di Inqitat, Dhofar (2016–2019), Egitto e Vicino Oriente, 2019; XLII, 121–135.
28. Newton L, Zarins J. Dhofar through the ages: an ecological, archaeological and historical landscape. Oxford: Archeopress; 2017.
29. Sridhar, T.S. Alagankulam. An Ancient Roman Port City of Tamil Nadu. Department of Archaeology Government of Tamilnadu; 2005.
30. Lischi S. From the Paleolitich to the Islamic Period: the History of Dhofar through the Archaeological Study of Inqitat. In: Cattani M, Frenez D, eds. Dreamers. 40 years of Italian archaeological research in Oman. Rome: BraDypUS; 2019. p. 149–51.
31. Nardella F, Landi N, Degano I, Colombo M, Serradimigni M, Tozzi C, Ribechini E. Chemical investigations of bitumen from Neolithic archaeological excavations in Italy by GC/MS combined with principal component analysis. Anal Methods. 2019;11:1449–59.
32. Łucejko J, Connan J, Orsini S, Ribechini E, Modugno F. Chemical analyses of Egyptian mummification balms and organic residues from storage jars dated from the Old Kingdom to the Copto-Byzantine period. J Archaeol Sci. 2017;85:1–12.
33. Whitbread IK. Fabric description of archaeological ceramics. In: Hunt A, ed. The Oxford handbook of archaeological ceramic analysis. Oxford: Oxford University Press; 2017. https://doi.org/10.1093/oxfordhb/9780199681532.013.13.
34. Pavan A. Khor Rori Report 3. A cosmopolitan city on the Arabian coast. The imported and local pottery from Khor Rori. Roma: L'ERMA di Bretschneider; 2017.
35. Terrell EE, Peterson PM, Wergin WP. Epidermal features and spikelet micromorphology in *Oryza* and related genera (Poaceae: Oryzeae). Smithsonian Contributions to Botany. 2001. https://doi.org/10.5479/si.0081024X.91.
36. Tomber R, Cartwright C, Gupta S. Rice temper: technological solutions and source identification in the Indian Ocean. J Archaeol Sci. 2011;38:360–6.
37. Riccardi MP, Messiga B, Duminuco P. An approach to the dynamics of clay firing. Appl Clay Sci. 1999;15:393–409.
38. Cultrone G, Rodriguez-Navarro C, Sebastian E, Cazalla O, De La Torre MJ. Carbonate and silicate phase reactions during ceramic firing. Eur J Mineral. 2001;13:621–34.
39. Maniatis Y, Tite MS. Technological Examination of Neolitliic-Bronze Age Pottery from Central and Southeast Europe and from Near East. J Archaeol Sci. 1981;8:59–76.
40. Piperno DM. Phytoliths: a Comprehensive Guide for Archaeologists and Paleoecologists. Lanham: AltaMira Press; 2006.
41. Hodson MJ, White PJ, Mead A, Broadley MR. Phylogenetic variation in the silicon composition of plants. Ann Bot. 2005;96:1027–46.
42. Mariotti Lippi M, Pallecchi P. Organic Inclusions. In: Hunt A, editor. The Oxford handbook of archaeological ceramic analysis. Oxford: Oxford University Press; 2017. p. 565–83.
43. Connan J, Nissenbaum A. The organic geochemistry of the Hasbeya asphalt (Lebanon): comparison with asphalts from the Dead Sea area and Iraq. Org Geochem. 2004;35:775–89.
44. Peters KE, Walters CC, Moldowan JM. The Biomarker Guide: Volume 2: Biomarkers and Isotopes in the Petroleum Exploration and earth History. Cambridge: Cambridge University Press; 2005.
45. Mello MR, Gaglianone PC, Brassell SC, Maxwell JR. Geochemical and biological marker assessment of depositional environments using Brazilian offshore oils. Mar Pet Geol. 1988;5:205–23.

Lischi *et al. Herit Sci*   (2020) 8:76

Page 14 of 14

46. Connan, J. Le bitume dans l'Antiquité. Paris Editions Errance; 2012.
47. El Diasty WS, Abo Ghonaim AA, Mostafa AR, El Beialy SY, Edwards KJ. Biomarker characteristics of the Turonian-Eocene succession, Belayim oilfields, central Gulf of Suez. Egypt. Journal of the Association of Arab Universities for Basic and Applied Sciences. 2016;19:91–100.
48. Summons RE, Jahnke LL, Hope JM, Logan GA. 2-Methylhopanoids as biomarkers for cyanobacterial oxygenic photosynthesis. Nature. 1999;400:554–7.
49. Hill DV, Speakman RJ, Glascock MD. Chemical and mineralogical characterization of Sasanian and early Islamic glazed ceramics from the Deh Luran plain, southwestern Iran. Archaeometry. 2004;46:585–605.
50. Rougeulle A. A medieval trade entrepot at Khor Rori? The study of the Islamic ceramics from Hamr Al-Sharqiya. In: Avanzini A, ed. A Port in Arabia between Rome and the Indian Ocean (3rd C. BC – 5th C. AD). Khor Rori Report 2. Roma: L'Erma di Bretschneider; 2008. p. 645–67.
51. Whitcomb DS, Johnson JH. Quseir al-Qadim 1978: Preliminary Report. Alexandria: American Research Center in Egypt Reports 1; 1979.
52. Mariotti Lippi M, Gonnelli T, Pallecchi P. Rice chaff in ceramics from the archaeological site of Sumhuram (Dhofar, Southern Oman). J Archaeol Sci. 2011;38:1173–9.
53. Miller N. Plant remains from Ville Royale II, Susa. Cahiers de la Délégation Archéologique Française en Iran. 1981;12:137–42.
54. Al-Jibouri BSM, Gayara AD. Paleocene sequence development in the Iraqi western desert. Iraqi Bulletin of Geology and Mining. 2015;11:1–18.
55. Munsell Color (Firm). Munsell Soil Color Charts: with Genuine Munsell Color Chips. Grand Rapids, MI: Munsell Color; 2010.

Publisher's Note

Springer Nature remains neutral with regard to jurisdictional claims in published maps and institutional affiliations.